

Radiation-pressure cooling and optomechanical instability of a micro-mirror

O. Arcizet, P.-F. Cohadon, T. Briant, M. Pinard, and A. Heidmann
Laboratoire Kastler Brossel, Case 74, 4 place Jussieu, 75252 Paris Cedex 05, France

PACS numbers:

Recent experimental progress in table-top experiments [1, 2] or gravitational-wave interferometers [3] has enlightened the unique displacement sensitivity offered by optical interferometry. As the mirrors move in response to radiation pressure, higher power operation, though crucial for further sensitivity enhancement, will however increase quantum effects of radiation pressure, or even jeopardize the stable operation of the detuned cavities proposed for next-generation interferometers [4, 5, 6]. The appearance of such optomechanical instabilities [7, 8] is the result of the nonlinear interplay between the motion of the mirrors and the optical field dynamics. In a detuned cavity indeed, the displacements of the mirror are coupled to intensity fluctuations, which modifies the effective dynamics of the mirror. Such "optical spring" effects have already been demonstrated on the mechanical damping of an electromagnetic waveguide with a moving wall [9], on the resonance frequency of a specially designed flexure oscillator [10], and through the optomechanical instability of a silica micro-toroidal resonator [11]. We present here an experiment where a micro-mechanical resonator is used as a mirror in a very high-finesse optical cavity and its displacements monitored with an unprecedented sensitivity. By detuning the cavity, we have observed a drastic cooling of the micro-resonator by intracavity radiation pressure, down to an effective temperature of 10 K. We have also obtained an efficient heating for an opposite detuning, up to the observation of a radiation-pressure induced instability of the resonator. Further experimental progress and cryogenic operation may lead to the experimental observation of the quantum ground state of a mechanical resonator [12, 13, 14], either by passive [15] or active cooling techniques [16, 17, 18].

The resonator is placed at the end of a linear cavity, along with a conventional coupling mirror (Fig. 1a). As we are only interested in the motion at frequencies Ω close to a resonance frequency Ω_m of the resonator, the mirror dynamics can be approximated as the one of a single harmonic oscillator, with resonance frequency Ω_m , mass M , damping Γ_m and mechanical susceptibility:

$$\chi_m[\Omega] = \frac{1}{M(\Omega_m^2 - \Omega^2 - i\Gamma_m\Omega)}. \quad (1)$$

The resonator is submitted to a radiation pressure force F_{rad} induced by the intracavity field. Depending on the detuning $\Psi \equiv 4\pi L/\lambda[2\pi]$, where L is the cavity length and λ the laser wavelength, any small displacement x of the resonator induces a variation of the intracavity power

P and of the radiation pressure (see Fig. 1b). As a consequence, the spring constant $k = M\Omega_m^2$ of the resonator is balanced by the radiation pressure force: for a positive detuning, the displacement creates a negative linear force and thereby an additional binding force, increasing the effective spring constant, whereas for a negative detuning, the force corresponds to a softening of the oscillator. Effects are null at resonance, maximum at half-width of the optical resonance, and proportional to the incident power. These effects have already been directly observed [10], as well as the bistable behaviour of the cavity for a negative detuning [19]. In our experiment, however, due to the high-finesse cavity and the high resonance frequency, such a static approach is no longer valid and one has to take into account the cavity storage time to evaluate the resonator dynamics. Additional dephasings appear and the radiation pressure force F_{rad} can be written in Fourier space [6]:

$$F_{\text{rad}}[\Omega] = -2\frac{\varphi\varphi_{\text{NL}}}{\Delta}M\Omega_m^2x[\Omega], \quad (2)$$

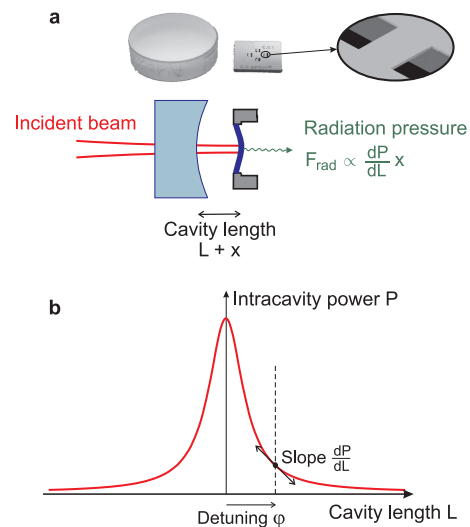


FIG. 1: Principle of radiation-pressure cooling. **a**, Layout of the optical cavity. The micro-resonator mirror is etched upon a 1 cm² silicon chip. The coupling mirror of the cavity is a standard low-loss silica mirror. **b**, Intracavity power P as a function of the cavity length L . Around a working point defined by the normalized cavity detuning φ , the force F_{rad} exerted by the intracavity field upon the micro-resonator is proportional to the slope of the Airy peak and to the displacement x of the resonator.

with

$$\Delta = (1 - i\Omega/\Omega_c)^2 + \varphi^2, \quad (3)$$

where $x[\Omega]$ is the Fourier component of the resonator displacement, $\varphi = \Psi/\gamma$ the detuning normalized to the cavity damping rate γ , and Ω_c the cavity bandwidth. φ_{NL} is a nonlinear phase-shift which characterizes the optomechanical coupling between the resonator and the light in the cavity. It corresponds to the normalized phase-shift of the cavity induced by the static recoil effect of the resonator [19] and is given by:

$$\varphi_{\text{NL}} = \frac{8\pi}{\lambda\gamma c} \frac{P}{M\Omega_m^2}. \quad (4)$$

At thermodynamical equilibrium, the equation of motion of the resonator is :

$$x[\Omega] = \chi_m[\Omega] (F_T[\Omega] + F_{\text{rad}}[\Omega]), \quad (5)$$

where F_T is the Langevin force responsible for the Brownian motion [20]. This equation of motion can be rewritten from (2) without the radiation pressure term, but with an effective mechanical susceptibility $\chi_{\text{eff}}[\Omega]$:

$$\chi_{\text{eff}}[\Omega]^{-1} = \chi_m[\Omega]^{-1} + 2\frac{\varphi\varphi_{\text{NL}}}{\Delta}M\Omega_m^2. \quad (6)$$

In the limit of a mechanical quality factor $Q = \Omega_m/\Gamma_m \gg 1$, $\chi_{\text{eff}}[\Omega]$ still has a lorentzian shape, but with effective resonance frequency and damping given by:

$$\Omega_{\text{eff}} = \Omega_m \left(1 + \text{Re}\frac{\varphi\varphi_{\text{NL}}}{\Delta}\right) \quad (7)$$

$$\Gamma_{\text{eff}} = \Gamma_m \left(1 - 2Q \text{Im}\frac{\varphi\varphi_{\text{NL}}}{\Delta}\right), \quad (8)$$

where Δ is now evaluated at the resonance frequency Ω_m . The Q factor in eq. (8) indicates a much stronger dependence of the damping upon radiation pressure effects as long as the imaginary part of $1/\Delta$ stays comparable to its real part, that is for $\Omega_m \simeq \Omega_c$. The radiation pressure effects can then increase or decrease the damping of the resonator, depending on the sign of the detuning. Since the Langevin force is not modified, one gets a situation somewhat similar to the one obtained by cold damping [16]: the system still obeys the fluctuation-dissipation theorem [20], but at a different effective temperature, given for small frequency shifts ($\Omega_{\text{eff}} - \Omega_m$) by:

$$\frac{T_{\text{eff}}}{T} \simeq \frac{\Gamma_m}{\Gamma_{\text{eff}}}. \quad (9)$$

Both radiation pressure cooling and heating can therefore be performed, depending on the sign of the cavity detuning. A similar result has recently been demonstrated with a silicon microlever, using the photothermal force rather than radiation pressure [15].

In our experiment (Fig. 2), a silicon doubly-clamped ($1\text{ mm} \times 1\text{ mm} \times 60\ \mu\text{m}$) beam with a mirror coated

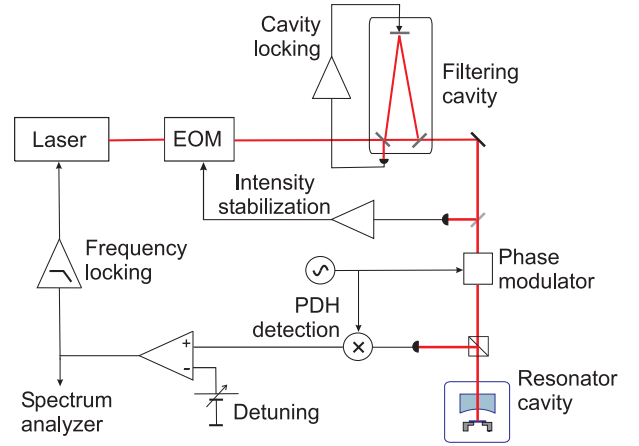


FIG. 2: Experimental setup used to monitor and to cool the micro-mechanical oscillator. A Nd:YAG laser ($\lambda = 1,064\text{ nm}$) is intensity-stabilized at low frequency with an electro-optic modulator (EOM) and spatially filtered before entering the micro-resonator cavity. The displacement signal is extracted by means of a Pound-Drever-Hall (PDH) phase modulation scheme using a resonant electro-optic phase modulator. The low-frequency part of the signal is used to lock the laser frequency around the cavity resonance, with a preset detuning given by a DC offset. The high-frequency part is used to monitor the resonator displacements.

upon its surface is used as back mirror of a single-ended Fabry-Perot cavity [17]. We use one particular vibration mode, which has the following characteristics: $\Omega_m/2\pi \simeq 814\text{ kHz}$, an effective mass $M = 190\ \mu\text{g}$, a spring constant $k \simeq 5 \times 10^6\ \text{N.m}^{-1}$, and a mechanical quality factor $Q = 10,000$ in vacuum (residual pressure below 10^{-2} mbar), with the whole vacuum chamber at room temperature $T = 300\text{ K}$. Both the quality of the low-loss dielectric coating and the low roughness of the resonator have allowed us to reach an optical finesse $\mathcal{F} = \pi/\gamma = 30,000$, with a cavity bandwidth $\Omega_c/2\pi = 1.05\text{ MHz}$ ($L = 2.4\text{ mm}$). Such a high finesse dramatically increases both the radiation pressure cooling effect and the sensitivity of the phase of the reflected field to the resonator displacements. Using a highly stabilized laser source and a Pound-Drever-Hall (PDH) phase modulation scheme has indeed allowed us to reach a sensitivity of $4 \times 10^{-19}\text{ m}/\sqrt{\text{Hz}}$ near the resonance frequency: the thermal peak of the resonator at room temperature is observed with a 50 dB signal-to-noise ratio with respect to the background thermal noise of the surrounding vibration modes.

The calibration of our setup is performed in two steps. First, the calibration is performed when the cavity is at resonance with a frequency modulation of the laser [2, 17]. Second, we have to take into account the lowering of the sensitivity for a non-zero detuning, which stems from two origins: the lower dependence of the phase response with cavity detuning away from resonance, and the distortion of the PDH signal for large detunings. For that purpose, we drive the resonator into motion (with

an amplitude $\simeq 10^{-13}$ m) with a modulated electrostatic force at 814 kHz and monitor the displacement signal for different detunings, and an incident power ($50 \mu\text{W}$) low enough to insure that radiation pressure has no effect. The observed modulation has been used to calibrate every spectrum observed.

Fig. 3 shows the thermal noise spectra obtained for negative detunings and a 5 mW incident beam (a), and for positive detunings and a 2.5 mW incident beam (b). In both cases, the black curve corresponds to the resonant situation $\varphi = 0$. This thermal noise spectrum (rms amplitude $\simeq 2.9 \times 10^{-14}$ m, driven by a $8 \times 10^{-25} \text{N}^2/\text{Hz}$ Langevin force spectral density) has been used to infer the value of the effective mass ($190 \mu\text{g}$) used throughout the paper. This value is in good agreement with a finite-element method (FEM) computation, which yields a value of $130 \mu\text{g}$ [17]. The discrepancy is accounted for by the overall accuracy of both the FEM computation and the fabrication of the micro-resonator, by the imperfect overlap of the vibration mode with a non-centered optical beam, and by the coupling of the mode with the ones of the wafer the resonator is engraved onto.

Both cooling and heating are evident on the noise spectra of Fig. 3. For a negative detuning, the spectra are both widened and drastically decreased at their resonance frequencies. The decrease of the area of the curves, which is directly related to the effective temperature by the equipartition theorem, is a strong indication of the temperature reduction. The situation is opposite for positive detunings, where the spectra are strongly narrowed and increased at resonance. The absence of any spurious noise in the spectra is due to both the high sensitivity of our experiment and the stable operation of the cavity. Note also in both cases the clear frequency shift ($\Omega_{\text{eff}} - \Omega_{\text{m}}$) of the resonances.

Our experimental results can be further tested by looking at the dependence of both the damping ratio $\Gamma_{\text{eff}}/\Gamma_{\text{m}}$ and the frequency shift $(\Omega_{\text{eff}} - \Omega_{\text{m}})/2\pi$ with respect to the detuning φ . Fig. 4a presents our experimental results, for five optical powers from 0.5 mW to 3.2 mW, along with the theoretical fits deduced from eqs. (7) and (8). Both are in very good agreement. The insert shows the intracavity power at resonance P , single free parameter derived from the preceding fits, as a function of the incident power P_{in} . It exhibits the expected linear dependence, with a slope $P/P_{\text{in}} = 2,970$ in agreement at the 1% level with the one deduced from cavity and insertion losses. This clearly shows that the observed cooling effect is solely due to radiation pressure. Indeed, with the estimated mirror absorption ($\simeq 3$ ppm), thermoelastic effects are expected to be 10^6 times lower. Bolometric effects [15] are difficult to estimate, but both the low absorption and the large thickness of the resonator still are in favor of a negligible effect. We have also performed the same experiment for other modes of the resonator, with the same excellent agreement with theory. In particular, a mode with a resonance frequency $\Omega_{\text{m}} = 2\pi \times 2,824$ kHz larger than the cavity bandwidth Ω_{c} exhibits a frequency

shift ($\Omega_{\text{eff}} - \Omega_{\text{m}}$) with an opposite sign, as expected from eqs. (3) and (7) for not too large detunings φ .

Figure 4b presents a color-chart of the dependence of the effective damping Γ_{eff} in the detuning/intracavity power plane. Experimental series of points were taken for fixed stabilized incident powers, following the Airy curves in the plane. The color code ranges from dark blue (for large Γ_{eff} and low T_{eff}) to red (for low Γ_{eff} and large T_{eff}). The green points (corresponding to $\Gamma_{\text{eff}} \simeq \Gamma_{\text{m}}$) are located at the resonance, at large detunings (where the slope of the Airy peak vanishes) and at low intracavity power (where radiation pressure effects are weaker). The highest cooling (dark blue) is obtained near a negative detuning $\varphi \simeq -0.6$ and for a high intracavity power P , whereas the largest heating effect (red) is obtained for a positive detuning. Gray curves correspond to equal effective dampings Γ_{eff} and the black one to $\Gamma_{\text{eff}} = 0$. Above this line, the resonator becomes unstable and starts to oscillate at its effective resonance frequency, as has already been demonstrated with a micro-toroidal resonator [11]. We have observed a similar effect, as shown on Figs. 4a and 4b, where the instability region is displayed with no adjustable parameter. Also note that the secondary peaks on the red spectrum of Fig. 3b (more than 50 dB below the resonance spectrum level) are due to the lower stability of the cavity operation close to the instability region. This is to our knowledge the first experimental demonstration of such a radiation-pressure instability in an open optical cavity.

Fig. 4c displays the variations of the effective temperature with the detuning φ . For a fixed input power of 3.2 mW, T_{eff} ranges from 20 K at an optimum detuning $\varphi \simeq -0.45$, to 2000 K for a positive detuning, very close to the instability region. The dependence with φ is well accounted for by our single oscillator theoretical model (eq. 9) for positive and negative but not too large detunings (dashed line). For larger negative detunings, the noise spectrum is so low that the thermal noise background due to other vibration modes of the resonator is no longer negligible: a slight modification of our model taking this background into account well depicts the characteristics of our experimental results (full line). Due to the low absorption of the micro-resonator, the residual discrepancy at large detuning (left point in Fig. 4c) cannot be related to a residual heating process. Furthermore, effective temperatures as low as 10 K have been obtained with a 12 mW incident beam.

Our experimental setup is the first high-sensitivity optical displacement sensor to show a direct effect of radiation pressure, an ubiquitous -though extremely weak- effect that every optical experiment will eventually be sensitive to. Further enhancement and low temperature operation of such a system may lead to the experimental demonstration of the quantum ground state of a mechanical resonator [12, 13, 14, 15, 17, 18]: radiation-pressure cooling is a fundamental process which eventually involves nothing but a mechanical oscillator in interaction with one cavity mode and its quantum fluctu-

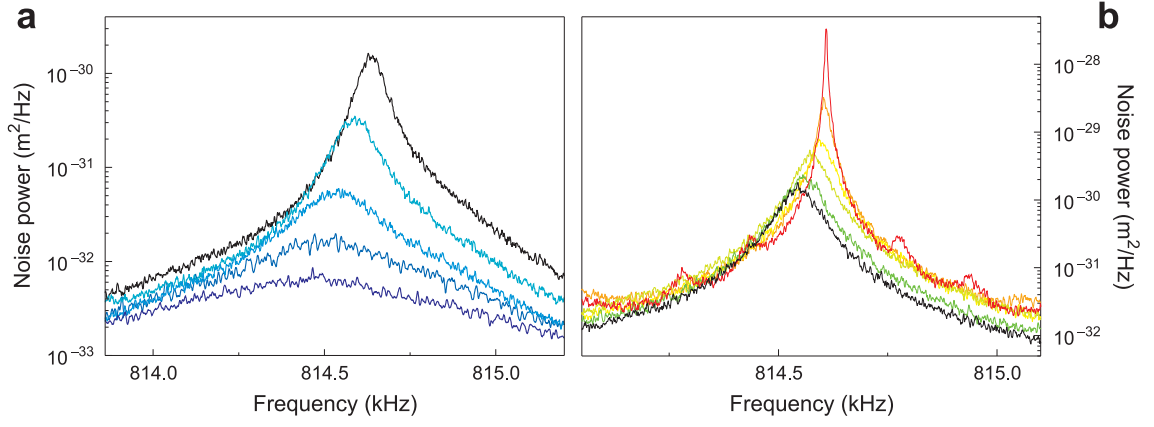


FIG. 3: Thermal noise spectra, normalized as micro-resonator displacements. Black curves correspond to $\varphi = 0$. **a**, Curves green to blue are obtained for negative detunings $\varphi = -0.1, -0.25, -0.4,$ and -0.6 , respectively, and for an incident power of 5 mW. **b**, Curves green to red are obtained for positive detunings $\varphi = 0.03, 0.06, 0.09, 0.11,$ and 0.13 , respectively, and for an incident power of 2.5 mW. The cooling and heating are evident through the area reduction or increase of these spectra. Note the related drift of the resonance frequency.

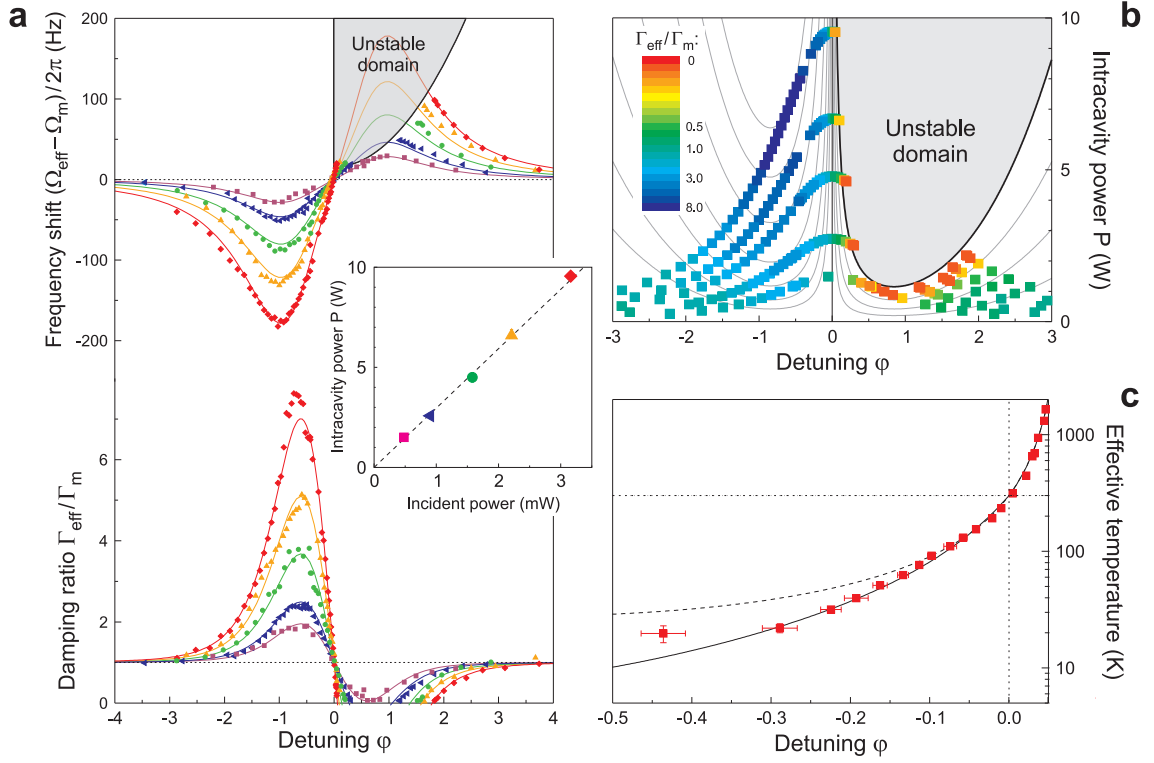


FIG. 4: Evolution of the cavity cooling and heating effects with respect to the detuning φ . **a**, Frequency shift $(\Omega_{\text{eff}} - \Omega_m)/2\pi$ (top) and damping ratio $\Gamma_{\text{eff}}/\Gamma_m$ (bottom), for five values of incident power: 0.5 mW (purple), 0.9 mW (blue), 1.6 mW (green), 2.2 mW (yellow) and 3.2 mW (red). Points are experimental results and full lines are fits obtained from eqs. (4), (7) and (8), by adjusting the intracavity power at resonance P for each curve. Inset: evolution of the adjusted intracavity power P with the incident power. The dashed line is the linear dependence expected from cavity and insertion losses, with no adjustable parameter. The shaded area in the upper curve shows the instability zone where Γ_{eff} vanishes. **b**, Color-chart of the evolution of the damping ratio $\Gamma_{\text{eff}}/\Gamma_m$ in the detuning/intracavity power plane $\{\varphi, P\}$, for the same measurements as in **a**. The value is color-coded from dark blue (large damping, low temperature) to red (low damping, high temperature). Gray curves are equal effective damping loci. Note the green points (unity damping ratio) at the resonance $\varphi = 0$ and the vicinity of the red points with the instability region (shaded area). **c**, Evolution of the effective temperature with the cavity detuning, for a 3.2 mW incident beam. Squares: experimental points with error bars (s.e.m.). The dotted line is the reference level at $T = 300$ K ($\varphi = 0$), the dashed line the fit with the single oscillator model of eq. (9), and the full line the fit with a model taking into account the out-of-resonance tails of other modes of the micro-resonator.

ations, yielding a reliable estimation of the cooling limit. Furthermore, our knowledge of the other modes' dynamical behavior [17] appears as a major issue on the road to the quantum ground state as their out-of-resonance tails will no longer be negligible for extreme cooling ratios. Other possible novel effects in quantum optics include the experimental demonstration of the Standard Quantum Limit [21, 22], radiation-pressure induced squeezing of light [23], Quantum Non Demolition measurements [24] or non-classical states of the resonator motion [25, 26].

Acknowledgements are due to L. Rousseau for the fabrication of the micro-resonator and to J.-M. Mackowski and his group for the optical coating of the resonator. This work was partially funded by EGO (collaboration convention EGO-DIR-150/2003 for a study of quantum noises in gravitational wave interferometers). Laboratoire Kastler Brossel is "Unité mixte de recherche du Centre National de la Recherche Scientifique, de l'École Normale Supérieure et de l'Université Pierre et Marie Curie".

-
- [1] Rugar, D., Budakian, R., Mamin, H.J. & Chui, B.W. Single spin detection by magnetic resonance force microscopy. *Nature* **430**, 329-332 (2004).
- [2] Hadjar, Y., Cohadon, P.-F., Aminoff, C.G., Pinard, M. & Heidmann, A. High-sensitivity measurement of mechanical Brownian motion. *Europhys. Lett.* **47**, 545-551 (1999).
- [3] Abbott, B. *et al.* Upper Limits on a Stochastic Background of Gravitational Waves. *Phys. Rev. Lett.* **95**, 221101 (2005).
- [4] Meers, B. Recycling in laser-interferometric gravitational-wave detectors. *Phys. Rev. D* **38**, 2317-2326 (1988).
- [5] Heinzl, G. *et al.* Experimental Demonstration of a Suspended Dual Recycling Interferometer for Gravitational Wave Detection. *Phys. Rev. Lett.* **81**, 5493-5496 (1998).
- [6] Arcizet, O., Briant, T., Heidmann, A. & Pinard, M. Beating quantum limits in an optomechanical sensor by cavity detuning. *Phys. Rev. A* **73**, 033819 (2006).
- [7] Pai, A., Dhurandar, S., Hello, P. & Vinet, J.-Y. Radiation pressure induced instabilities in laser interferometric detectors of gravitational waves. *Eur. Phys. J. D* **8**, 333-346 (2000).
- [8] Zhao, C., Ju, L., Degallaix, J. & Blair, D. Parametric Instabilities and Their Control in Advanced Interferometer Gravitational-Wave Detectors. *Phys. Rev. Lett.* **94**, 121102 (2004).
- [9] Braginsky, V.B., Manukin, A.B. & Tikhonov, M.Yu. Investigation of dissipative ponderomotive effects of electromagnetic radiation. *Sov. Phys. JETP* **31**, 829-830 (1970).
- [10] Sheard, B.S., Gray, M. B., Mow-Lowry, C.M., McClelland, D.E. & Whitcomb, S.E. Observation and characterization of an optical spring. *Phys. Rev. A* **69**, 051801 (2004).
- [11] Kippenberg, T. *et al.* Analysis of Radiation-Pressure Induced Mechanical Oscillation of an Optical Microcavity. *Phys. Rev. Lett.* **95**, 033901 (2005).
- [12] Huang, X.M.H., Zorman, C.A., Mehregany, M. & Roukes, M.L. Nanoelectromechanical systems: Nanodevice motion at microwave frequencies. *Nature* **421**, 496 (2003).
- [13] Knobel, R.G. & Cleland, A.N. Nanometre-scale displacement sensing using a single electron transistor. *Nature* **424**, 291-293 (2003).
- [14] LaHaye, M.D., Buu, O., Camarota, B. & Schwab, K.C. Approaching the Quantum Limit of a Nanomechanical Resonator. *Science* **304**, 74-77 (2004).
- [15] Hohberger Metzger, C. & Karrai, K. Cavity cooling of a microlever. *Nature* **432**, 1002-1005 (2004).
- [16] Cohadon, P.-F., Heidmann, A. & Pinard, M. Cooling of a mirror by radiation pressure. *Phys. Rev. Lett.* **83**, 3174-3177 (1999).
- [17] Arcizet, O. *et al.* High-sensitivity optical monitoring of a micro-mechanical resonator with a quantum-limited optomechanical sensor. Preprint at: <<http://arxiv.org/quant-ph/0605174>> (2006).
- [18] Cohadon, P.-F., Arcizet, O., Briant, T., Heidmann, A. & Pinard, M. Optical monitoring and cooling of a micro-mechanical oscillator to the quantum limit. *SPIE Proceedings* **5846**, 124-134 (2005).
- [19] Dorsel, A., McCullen, J.D., Meystre, P., Vignes, E. & Walther, H. Optical Bistability and Mirror Confinement Induced by Radiation Pressure. *Phys. Rev. Lett.* **51**, 1550-1553 (1983).
- [20] Kubo, R. The fluctuation-dissipation theorem. *Rep. Prog. Phys.* **29**, 255-284 (1966).
- [21] Caves, C.M. Quantum-mechanical noise in an interferometer. *Phys. Rev. D* **23**, 1693-1708 (1981).
- [22] Jaekel, M.T. & Reynaud, S. Quantum limits in interferometric measurements. *Europhys. Lett.* **13**, 301-306 (1990).
- [23] Fabre, C. *et al.* Quantum-noise reduction using a cavity with a movable mirror. *Phys. Rev. A* **49**, 1337-1343 (1994).
- [24] Heidmann, A., Hadjar, Y. & Pinard, M. Quantum non-demolition measurement by optomechanical coupling. *Appl. Phys. B* **64**, 173-180 (1997).
- [25] Bose, S., Jacobs, K. & Knight, P.L. Preparation of non-classical states in cavities with a moving mirror. *Phys. Rev. A* **56**, 4175-4186 (1997).
- [26] Pinard, M. *et al.* Entangling movable mirrors in a double-cavity system. *Europhys. Lett.* **72**, 747-753 (2005).